Development 126, 3735-3745 (1999)
Printed in Great Britain © The Company of Biologists Limited 1999
DEV2434

Ontogeny and behaviour of early macrophages in the zebrafish embryo

Philippe Herbomel[1,*], Bernard Thisse[2] and Christine Thisse[2]

[1]Unité de Biologie Moléculaire du Développement, URA1947 du CNRS, Département de Biologie Moléculaire, Institut Pasteur, 25 rue du Dr Roux, 75724 Paris Cedex 15, France
[2]Institut de Génétique et de Biologie Moléculaire et Cellulaire, CNRS/INSERM/ULP, BP163, 67404 Illkirch Cedex, CU de Strasbourg, France

*Author for correspondence at present address: Unité de Génétique des Déficits Sensoriels, Département des Biotechnologies, Institut Pasteur, 25 rue du Dr Roux, 75724 Paris Cedex 15, France (e-mail: herbomel@pasteur.fr)

Accepted 16 June; published on WWW 5 August 1999

SUMMARY

In the zebrafish embryo, the only known site of hemopoieisis is an intra-embryonic blood island at the junction between trunk and tail that gives rise to erythroid cells. Using video-enhanced differential interference contrast microscopy, as well as in-situ hybridization for the expression of two new hemopoietic marker genes, *draculin* and *leucocyte-specific plastin*, we show that macrophages appear in the embryo at least as early as erythroid cells, but originate from ventro-lateral mesoderm situated at the other end of the embryo, just anterior to the cardiac field. These macrophage precursors migrate to the yolksac, and differentiate. From the yolksac, many invade the mesenchyme of the head, while others join the blood circulation. Apart from phagocytosing apoptotic corpses, these macrophages were observed to engulf and destroy large amounts of bacteria injected intravenously; the macrophages also sensed the presence of bacteria injected into body cavities that are isolated from the blood, migrated into these cavities and eradicated the microorganisms. Moreover, we observed that although only a fraction of the macrophage population goes to the site of infection, the entire population acquires an activated behaviour, similar to that of activated macrophages in mammals. Our results support the notion that in vertebrate embryos, macrophages endowed with proliferative capacity arise early from the hemopoietic lineage through a non-classical, rapid differentiation pathway, which bypasses the monocytic series that is well-documented in adult hemopoietic organs.

Key words: Hematopoiesis, Macrophage, DIC video-microscopy, Zebrafish, Yolksac, Lateral mesoderm, Head mesoderm, Phagocytosis, L-plastin, Draculin

INTRODUCTION

The zebrafish embryo has recently become one of the major model organisms for the study of vertebrate embryogenesis. Its transparency is one of its main assets, allowing one to view the details of embryological processes in the live embryo, using Differential Interference Contrast (DIC, or 'Nomarski') microscopy. This tool, together with single-cell tracing experiments using fluorescent dyes, has produced a fairly comprehensive description of zebrafish embryogenesis (Kimmel et al., 1995).

We recently found that when further improved by video-enhancement (Hayden and Allen, 1984), DIC microscopy can give access to a host of previously unapproached details of cell behaviours and even intracellular life in the zebrafish embryo, and reveal unknown aspects of vertebrate embryogenesis. The present paper describes the ontogeny and functional properties of a primitive macrophage lineage in the early zebrafish embryo.

MATERIALS AND METHODS

DIC video-microscopy

Embryos were observed under a coverslip in a depression slide filled with Volvic mineral water containing 0.02% tricaine to prevent embryo twitching. For dorsal viewing during somitogenesis, the embryos were embedded in 0.5% agarose in embryo medium (Westerfield, 1995). Embryos were viewed with a Reichert Polyvar 2 microscope equipped with DIC optics, using ×40 and ×100 oil immersion objectives. Images were captured by a Hitachi HV-C20 tri-CCD colour video camera, in which all contrast-dampening functions were set off, so that with the ×100 objective the final magnification on a 26-cm video screen was ×4000 with excellent contrast, allowing, for instance, sight of mitochondria and intracellular vesicle trafficking in the embryo.

Video-sequences were recorded from the Y/C output of the camera either by a Panasonic AG6730 time-lapse tape recorder in S-VHS format, or by a Sony DHR1000 tape recorder in Digital Video (DV) format. Single video images were captured and stored on a PC from the DV videotapes, through the Sony DVK2000 capture board. Digitized images were then processed with the Adobe Photoshop IV software.

Since DIC optics has a characteristically small depth of field, overall pictures of cells spread on a curved surface such as that of the yolkball (Figs 3-5) were obtained by fusing several overlapping pictures obtained at slightly different foci, using the Adobe Photoshop IV software.

Cell labelling in vivo

Single-cell labelling of 16-cell embryos with 2 mDa Dextran-Texas Red (Molecular Probes) was done according to Strehlow et al. (1994).

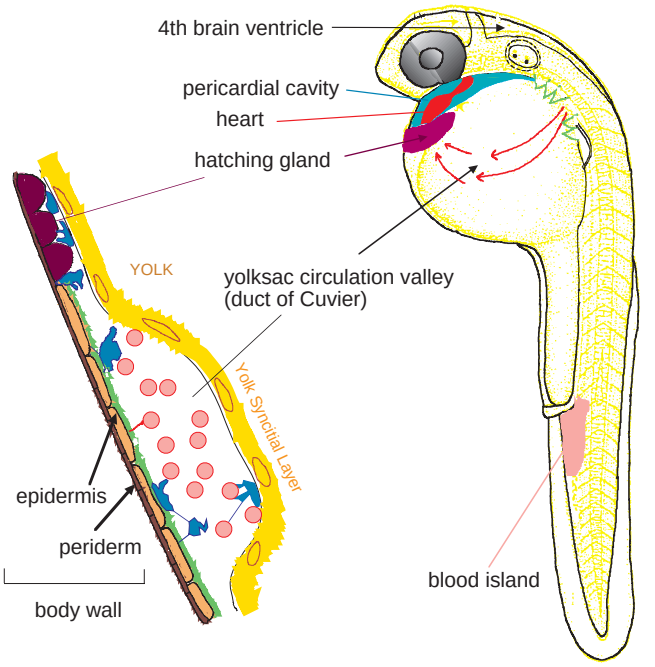

Fig. 1. Relevant landmarks in the day2 zebrafish embryo. (Right) Lateral view showing the pericardial cavity (light blue), heart (red), hatching gland (purple) and blood island (pink). At this stage (29 hpf), proerythroblasts have already left the blood island. Red arrows on the yolksac indicate venous blood flow in a depression of the yolk surface designated here as the 'yolksac circulation valley' (duct of Cuvier in most other fish, but here no vessel encloses the blood). (Left) Diagram of a section of the yolksac centered on the circulation valley, showing the yolk, released to the embryo by a syncitial layer (yellow), erythroblasts (pink), macrophages (blue), periderm (dark brown), epidermis (light brown) and its basal lamina (green).

cDNA clones and whole-mount in situ hybridization

The nucleotide sequences of the cDNAs encoding zebrafish draculin and L-plastin are available from GenBank under accession numbers AF157109 and AF157110, respectively. Whereas draculin appears to be a new zinc-finger protein with no homolog in sequence databases, our zebrafish *L-plastin* cDNA encodes the 200 C-terminal amino acids of a protein displaying 79% identity to the homologous portion of human L-plastin. The *flk-1* cDNA clone was kindly provided by L. Sumoy and D. Kimelman.

Whole-mount in situ hybridization was performed according to Thisse et al. (1993). The fully detailed protocol is accessible on the web at the *zfin* server: http://www-igbmc.u-strasbg.fr/zf_info/zfbook/chapt9/9.82.html.

Injection of bacteria in day2 embryos

The strains used were *E. coli* K12 DH5 and *B. subtilis* W168. For intravenous injections, we injected a few nl of a 4× concentrated stationary phase bacterial culture grown overnight, supplemented with 1% Phenol Red to help visualize the injection process, into the axial vein, close to the urogenital opening. Injections in the pericardial cavity or fourth ventricle of the brain were done using the same type of bacterial culture, except that it was not further concentrated 4×.

RESULTS

In the zebrafish, blood circulation starts around 25 hours post-fertilization (hpf). Unlike most fish embryos, the venous blood stream is not contained in any vessel as it approaches the heart; it flows freely over the lateral sides of the yolk, and these two streams join anteriorly to enter the heart (Fig. 1).

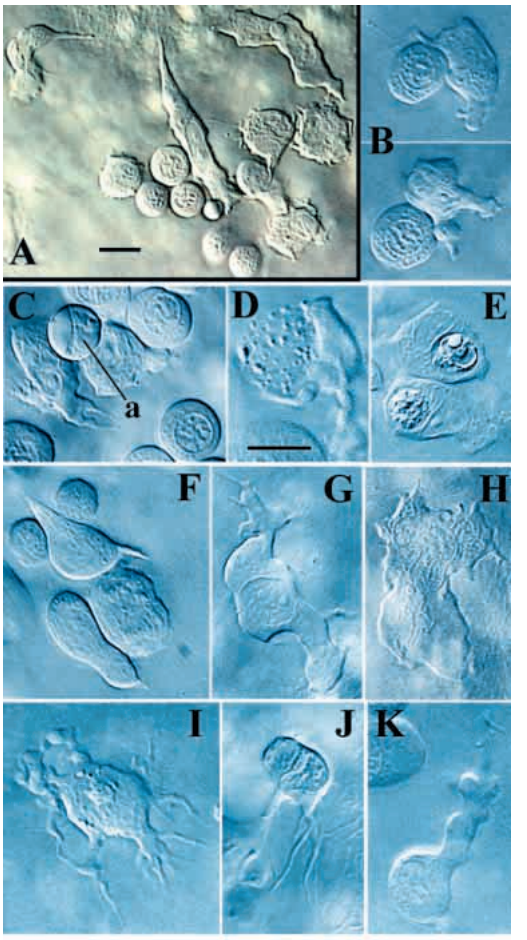

Fig. 2. Macrophages in the yolksac circulation valley of the day2 embryo. (A) Macrophages and erythroblasts just outside the main yolksac blood stream, 29 hpf. Erythroblasts are smaller, rounded cells with a circular nucleus and a smooth contour. Bar, 10 μm. (B-K) Higher magnification views. (B) close interaction of two macrophages with two erythroblasts at 26 hpf. (C) Erythroblasts and macrophages before the onset of blood circulation; a, apoptotic erythroblast. (D) A frustrated macrophage, trying to phagocytose an apoptotic 'bubble'. (E) Two macrophages containing remnants of apoptotic corpses. (F) A dividing macrophage, in anaphase B, in contact with two other macrophages. The two smaller cells on either side of the uppermost macrophage are sister erythroblasts just arisen from a mitosis. (G-K) Various macrophage morphologies, which tend to be adopted collectively by macrophages in the same vicinity. Scale bars, 10 μm.

A closer look at these blood streams reveals that a fraction of blood cells stop over the yolk, either on the sides of the blood stream or within it, and resist the flow. At higher magnification, two cell types become clear: erythroblasts, as expected, but also amoeboid cells with bean-shaped eccentric nuclei (Fig. 2), some of which contain phagocytic vacuoles (Fig. 2E). High-resolution time-lapse DIC video-microscopy reveals their ever-changing shapes, which can quickly switch from rounded to highly sculpted and vice versa. Fig. 2 shows a selection, although no single plane of focus captures their often exuberant three-dimensional shapes.

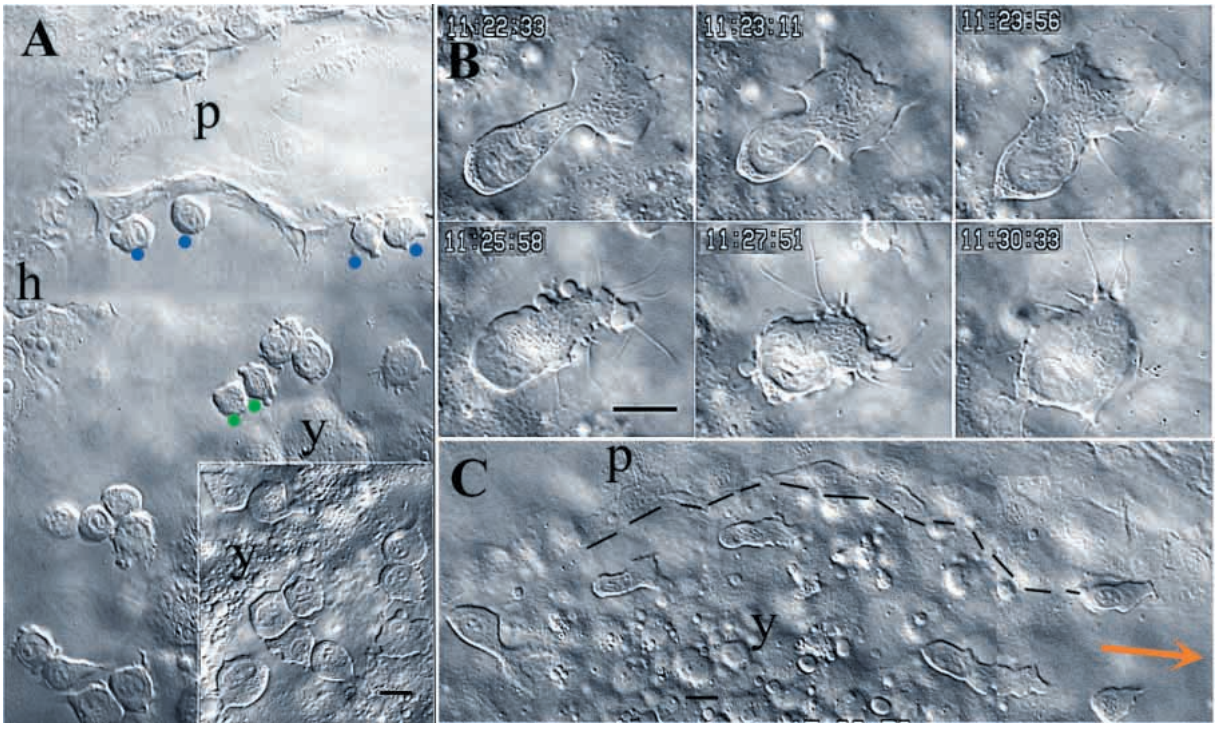

Fig. 3. Young macrophages in the anterior yolksac, before the arrival of erythroblasts. (A) 26-somite stage; the lateral boundary of the pericardial envelope (p) is outlined by a single line of fibroblast-like cells, which we call the pericardial hinge. Blue dots designate four pre-macrophages along that hinge. The other pre-macrophages are under the hatching gland (h), part of which is visible on the left side of the picture, due to the curvature of the yolkball (y), which brings into focus increasingly superficial structures as one goes from the centre to the periphery. Green dots indicate two sister cells that just separated after mitosis. The bottom right inset shows another embryo of the same stage, in which pre-macrophages spread a little more - a possible transition towards the young macrophage state. (B) 28-somite stage. Selected instants within 8 minutes of the wandering of a young macrophage on the basal lamina of the epidermis, near the hatching gland. (C) 29-somite stage: six young macrophages wandering towards what will soon be the entry site of the proerythroblasts on the yolksac (slightly off the picture, in the direction indicated by the orange arrow). A dotted line underlies the pericardial hinge. Bars, 10 μm (same magnification in A and C).

With DIC video-microscopy, we have observed these amoebocytes phagocytosing the corpses or debris from apoptotic erythroblasts in the bloodstream. This behaviour, together with their morphological similarities to macrophages of mammals, qualify these amoebocytes as macrophages. They also show another typical trait of macrophages: a behaviour called ‘frustrated phagocytosis’ (Cannon and Swanson, 1992). So far studied in cultured mammalian cells, this phenomenon occurs naturally in the zebrafish embryo. Apoptotic erythroblasts sometimes inflate to a size larger than the original cell. When a macrophage sticks to such an apoptotic ‘bubble’, it tries to engulf it, unsucessfully for the prey is too big (Fig. 2D).

These macrophages resist the blood stream by anchoring either to the underlying yolk surface (i.e. the plasma membrane of the yolk syncitial layer) or, most often, to the basal lamina of the overlying ectoderm (a thin epidermal layer, itself overlain by a still thinner, protective epithelium, the periderm, see Fig. 1). They stop many erythroblasts that they touch, and then release them back into circulation, often after a close and lengthy interaction (Fig. 2B).

Macrophage development in the yolksac precedes the arrival of erythroblasts

What are the embryonic origins of these early macrophages? They clearly do not originate from the blood island at the trunk/tail boundary, which only provides endothelial cells and proerythroblasts that migrate to the yolksac by 24 hpf (Rieb, 1973; Al-Adhami and Kunz, 1977; Detrich et al., 1995).

We found that several hours before proerythroblast migration, macrophages are already on the anterior yolk, most of them under the hatching gland and along the pericardium (Fig. 3). By 26 somites, each embryo has 80-150 such macrophages, which display two types of morphologies. Some are half-spread and wandering, under the hatching gland and neighbouring epidermis. Fig. 3B shows one of these, rapidly interconverting between spread and more condensed shapes, and bristling with pseudopodia and filopodia. The second type are unspread, rounded cells of homogeneous size (12 μm in diameter), with little cytoplasm, and a typical crown of small blebs (Fig. 3A), which time-lapse recordings show to be highly dynamic. These cells divide frequently, and sooner or later become wandering young macrophages.

By the 29-somite stage, just before proerythroblasts arrive on the yolk, the seemingly random wandering of some young macrophages becomes oriented towards the site of arrival of the proerythroblasts. Several literally meet the proerythroblasts at their entry site (Fig. 3C). Upon meeting, erythroblasts and about one third of the macrophages (about two thirds remain under the hatching gland) interact for approximately 1 hour on the lateral yolksac (Fig. 2C). Then blood circulation slowly begins, taking away erythroblasts and some macrophages, which are then observed in vessels throughout the body (data not shown).

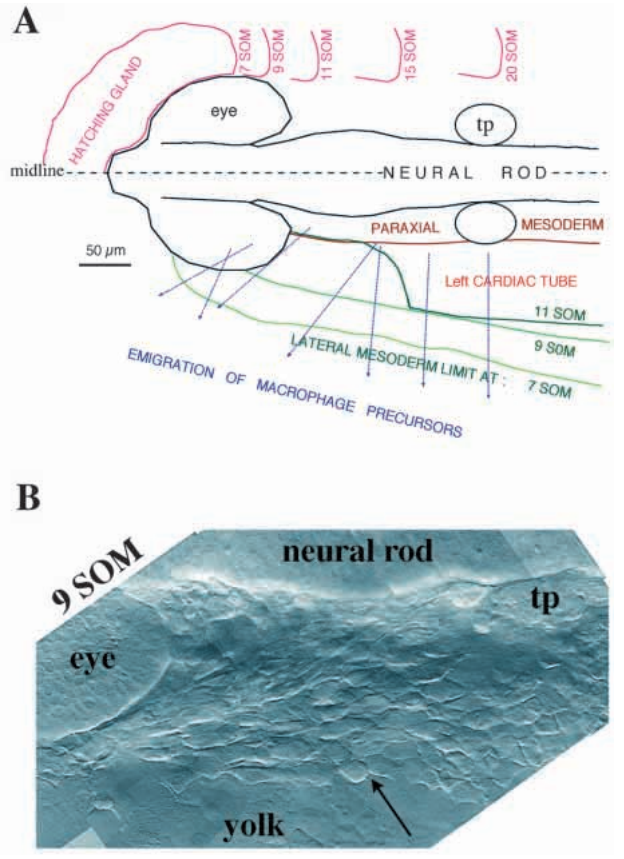

Fig. 4. Convergence of anterior lateral mesoderm to the body axis, and directions of emigration of macrophage precursors. (A) Diagram of a 9- to 11-somite embryo, in dorsal view. On the lower side, i.e. the left side of the embryo, progressively darker shades of green indicate the lateral boundary of the lateral mesoderm at the 7-, 9- and 11-somite stages. Blue arrows show the observed directions of emigration of macrophage precursors on the surface of the yolkball from the 13-somite stage onwards. Emigration from the more posterior zone medial to the cardiac tube starts later, around the 17-somite stage. For the sake of clarity, we indicated on the other (right) side of the embryo the posterior extension of the bilaterally symetrical hatching gland at successive developmental stages, showing that much of the emigration and accumulation of macrophage precursors takes place under the hatching gland. tp, trigeminal ganglion placode. (B) In this 9-somite embryo viewed dorsally, which was followed by video time-lapse recording up to 14-somites, the arrow shows the precise transition point between the future cardiac territory (to the right), which will not converge further, and the more anterior lateral mesoderm (to the left), which will converge to the midline within the next 2 hours.

Unlike monocyte-derived macrophages in mammals, these macrophages are still able to divide (Fig. 2F).

Yolksac macrophages originate from ventro-lateral mesoderm anterior to the heart

Through time-lapse video sequences taken at progressively earlier times, we traced the origin of the yolksac macrophages from the anteriormost lateral mesoderm of the head.

Fig. 4A shows our mapping by DIC microscopy of the relevant tissue boundaries in the head during the 7- to 15-somite period. Up to 9-somites, the lateral mesoderm, lying on the yolk surface, is converging homogeneously towards the midline. It is about three cells thick, with most cells roughly aligned with the body axis (Fig. 4B). At 9-somites, a sharp transition occurs. Lateral mesoderm cells more than 100 µm posterior to the eye (Fig. 4A and arrow in Fig. 4B) stop converging, and rapidly acquire an unmistakable morphology, with two layers of quite typical flat cells (Fig. 5A), an arrangement that will soon give rise to the cardiac tubes (one on each side of the embryo). In contrast, more anterior lateral mesoderm continues to converge, so that it lies entirely beneath paraxial mesoderm an hour later (11-somites, Fig. 4A). In some embryos, some of the most lateral cells lag behind this movement, and even start migrating in the reverse direction, towards the yolksac (data not shown). By the 13-somite stage, the bulk of macrophage progenitors begin to emigrate from beneath the paraxial mesoderm anterior to the cardiac field, creeping on the yolk, directly below the hatching gland. They often emigrate in lines of cells, each linked to the next (Fig. 5). This migration process lasts for several hours, up to at least the 26-somite stage. Starting at the 17-somite stage, this area of emigrating cells extends more posteriorly and macrophage progenitors are now seen emigrating on the yolk surface beneath the cardiac tubes (Fig. 5D-F). This process continues as the two cardiac tubes converge and fuse medially to form the heart and pericardial envelope (20-24 somite period).

Thus during the 14- to 30-somite time period, emigrated cells progressively accumulate as young macrophages on the anterior aspect of the yolksac, mainly under the hatching gland and along the lateral borders of the pericardial envelope.

Macrophages originate from the ventral side of the early gastrula

Our DIC microscopic observations suggested that macrophage precursors could originate from that anterior lateral mesoderm which, unlike the cardiac tubes precursors, converged further towards the midline an hour earlier, and disappeared below the paraxial mesoderm. To determine if macrophage precursors derive from axial, paraxial or lateral mesoderm, we used lineage tracing. Lateral mesoderm arises from the ventral side of the early gastrula. To simply distinguish between a ventral versus dorsal origin of macrophages, we injected a high molecular weight fluorescent cell tracer (2 mDa Dextran-Texas Red) into one of the peripheral blastomeres of 16-cell stage embryos. It has been shown that single blastomeres labeled at this stage usually give rise to tissues restricted to either the ventral or dorsal side of the early gastrula (Strehlow et al., 1994). Selecting injected embryos with this segregation of the lineage tracer, we found that while no dorsally labelled embryos (n=21) had any fluorescent macrophages, 15 out of 22 ventrally labelled embryos had at least 20% of the yolksac macrophages labelled (Figs 6, 7).

Thus early macrophages have a ventral origin in the early gastrula, like erythroblasts and heart cells, implying that their migratory route during gastrulation resembles that of heart precursors. 9 out of the 15 macrophage-positive embryos also had labeled cells in the heart, whereas 8 out of the 19 erythroblast-positive embryos did so (Fig. 6).

Early macrophage ontogeny can be traced by two successively expressed genes: *draculin* and *leucocyte-specific plastin*

We used the expression of two genes, *draculin* and *L-plastin*,

as markers for the ontogeny of early macrophages, from the late blastula stage throughout segmentation and organogenesis.

Both genes were isolated from a systematic in situ expression screen designed to identify genes involved in the early patterning of the zebrafish embryo (C. T. and B. T., unpublished data). Analysis of the predicted amino acid (aa) sequence of the *draculin* (*dra*) cDNA revealed that it codes for a 411-aa-long, poly(zinc finger) protein, containing 13 C_2H_2-type zinc fingers, preceded by 37 aa at the amino terminus, and 17 aa at the carboxy terminus (data not shown). These amino- and carboxy-terminal domains show no similarity to any sequences in available databases. *Dra* starts to be expressed at the late blastula stage all around the blastoderm margin. At the onset of gastrulation, *dra* expression becomes restricted to the ventral mesoderm territory, the presumptive prechordal plate, and the most dorso-marginal cells of the organizer (data not shown). Later in gastrulation, the dorso-marginal expression disappears, expression in the prechordal plate becomes restricted to its lateral rims, and the ventral mesoderm continues to express *dra* strongly (Fig. 8A,B). Expression persists as these cells form the lateral mesoderm all along the antero-posterior axis of the embryo (Fig. 8C). At the 3-somite stage (Fig. 8C,D,G), *dra* expression becomes stronger in two domains of the lateral mesoderm: a caudal domain, which marks the erythroid lineage, with the same location and dynamics as described for *GATA-1*, a marker of that lineage (Detrich et al., 1995), and a cephalic domain abutting anteriorly the hatching gland primordium (the main derivative of the prechordal plate). These two domains become more sharply defined as all other lateral mesoderm cells cease to express *dra*. At the 8- to 10-somite stages, the anterior domain consists of two thin bands of cells (Fig. 8H), which when compared with Nomarski views of live embryos at the same stage, are clearly cells of the most lateral mesoderm, precisely between the eye and hatching gland anteriorly and the cardiac primordia posteriorly (this was also confirmed by double in-situ hybridization for *dra* and the cardiac marker *nkx2.5*; not shown). Then the cephalic and caudal domains both converge rapidly to the midline. The two sides of the caudal domain fuse at the midline in the antero-posterior sequence typical of erythroid progenitors (Fig. 8E,F). Anteriorly, at 10-11 somites the left and right sides of the cephalic domain start expressing *dra* more strongly and no longer converge as two parallel bands, but as two patches that coalesce at the midline at 15-somites (Fig. 8I,J). During this process, an increasing proportion of these *draculin*-positive cells are found scattered as single cells, at increasing distances from the midline. Once the two patches have coalesced at the midline, this scattering continues to expand anteriorly and laterally, in a pattern indistinguishable from that described above for living macrophage precursors. The fact that the scattering has already begun by 11-somites, before any of these cells has reached the midline, implies that macrophage precursors do not need to reach the midline before emigrating

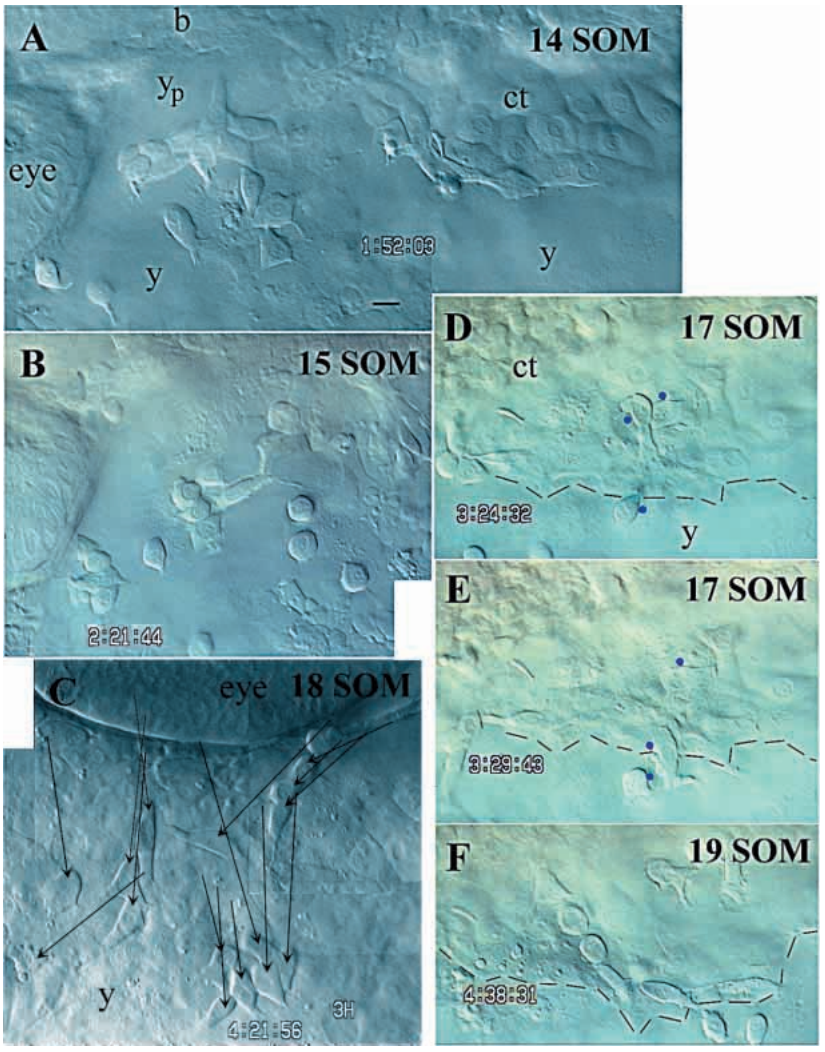

Fig. 5. Emigration of macrophage precursors from the ventral mesoderm to the yolksac. (A,B,D-F) Dorsal views of an individual embryo, between the 14- and 19-somite stages (medial up, anterior to the left). (A) At the 14-somite stage, cells present on the yolk surface (y) between the eye and cardiac tube (ct), are emigrating from the post-optic ventral mesoderm towards the anterior yolksac. y_p denotes the part of the yolk surface just lateral to the brain (b) that lies beneath paraxial mesoderm, itself out of focus because it is more dorsal. (B) The same embryo 30 minutes later, showing progression of the emigration. On the left, a group of four emigrating cells have just emerged from beneath the eye. (C) In another embryo, a lateral view shows the emigration of cells in the region lateral to the eye; while the picture is taken at 18-somites, arrows link each cell to its position 30 minutes earlier. (D-F) Same embryo as in A,B; at the 17-somite stage, cells begin to emigrate on the yolk surface beneath the cardiac tubes, the lateral limit of which is indicated by a dotted line. (D) Blue dots point at a macrophage precursor that just emerged laterally from below the cardiac tube, and at two others which are still under it (the other visible cells to the right are cardiac cells that slightly bulge out of the cardiac tube). (E) In the next 5 minutes, the second of the latter three macrophage precursors migrates rapidly out of the cardiac zone, joining the first emigrated one. (F) 1 hour later, a string of at least six cells is now emigrating beneath the cardiac tube towards the yolksac. Bar, 10 μm.

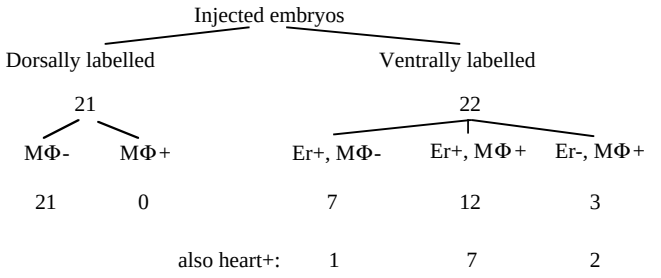

Fig. 6. Segregation of macrophage labelling with ventral labelling in embryos single-cell labelled at the 16-cell stage. The tissues considered as strictly ventral were: erythroblasts, pronephric duct, heart, yolk epidermis. Those considered as strictly dorsal were the hatching gland, trunk notochord, neural floor plate. The embryos classified as dorsally labelled were positive for at least one of these dorsal structures, and for none of the ventral structures. The converse criterium defined the ventrally labelled embryos. Other tissues known to be of more ventral (otocyst, lateral line, neural crest) or more dorsal (brain, head endothelium) origin correlated quite well with the above classification. 45 embryos were injected; in addition to the 43 clearly ventrally or dorsally labelled embryos presented above, 2 embryos showed a purely ventro-lateral labelling (otocyst+, neural crest+). Both were MΦ–. Er, erythroblasts; MF, macrophages.

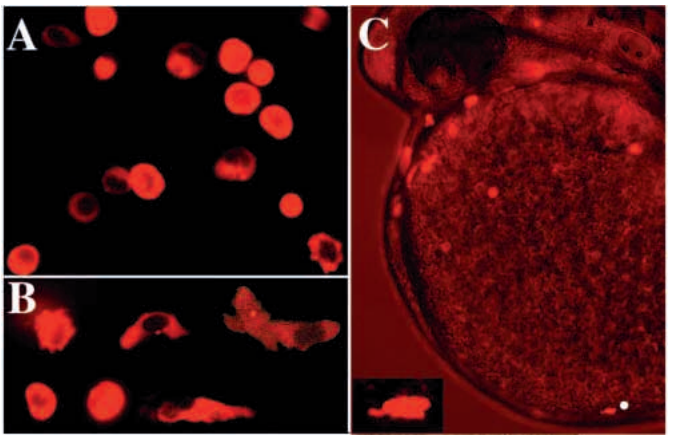

Fig. 7. Single-cell labelling in the 16-cell embryo reveals that macrophages originate from the ventral side of the early gastrula, as erythroblasts and heart cells. (A) 25 hpf: erythroblasts and macrophages both labelled in an embryo single-cell labelled with 2 mDa Dextran-Texas Red at the 16-cell stage. (B) Selection of labelled macrophages; (C) low-magnification view of a labelled embryo showing several labelled heart cells and yolksac macrophages (most out of focus, due to yolk curvature), one of which, indicated by a white dot, is shown enlarged in the lower left corner of the picture.

to the yolksac. Once on the yolksac, they progressively stop expressing *dra*, and this occurs much more quickly in cells on the right side than in those on the left (Fig. 8K).

The *flk-1* gene, an early marker of endothelial differentiation, is also expressed in the cephalic lateral mesoderm during the period studied here (Fouquet et al., 1997). We found that by 7-10 somites, *flk* is expressed anteriorly like *dra*, in two thin bands anterior to the heart field (data not shown). In the 10-15 somite period, the *flk* and *dra* expression patterns become increasingly distinct,with *flk*-expressing cells soon delineating the bilateral primordia of the arterial head vasculature (Fig. 8M-P). Double in-situ hybridization reveals that at 15 somites (Fig. 8P), the two patches of *dra*-expressing cells coalesce precisely between the two groups of *flk*-expressing cells that most likely represent the aortic arch primordia (Fouquet et al., 1997).

By 20-24 hpf, the posterior domain of *dra* expression becomes the embryonic erythroid blood island centered above the uro-genital opening; *dra* is strongly expressed in proerythroblasts. As these mature into circulating erythroblasts, they still express *dra*. Then *dra* expression in the blood progressively ceases to be detectable by 48 hpf, as erythroblasts become mature erythrocytes (data not shown).

L-plastin expression and further deployment of early macrophages from the yolksac

To follow later stages of macrophage development we analyzed expression of the zebrafish homolog of L-plastin (see Materials and Methods). L-plastin is an actin-bundling protein which, in the mouse, is specifically expressed in leukocytes, and is involved in their adhesion and activation. As macrophage precursors migrate to the yolksac, they start to express the *L-plastin* gene (Fig. 8L), and continue to express it as they mature (Fig. 8Q-T).

After their initial accumulation in the anterior part of the yolksac, young macrophages not only join the yolksac circulation valley (Fig. 1), but individually disperse on various tissue surfaces of the yolksac outside the blood flow (Fig. 8Q,S). Many others creep on the basal lamina of the ectoderm and join the head of the embryo, where they colonize the mesenchymal spaces and tissues (Fig. 8R-T, and data not shown). This process starts by the 26-somite stage, and leads to about 100 macrophages in the head at 36 hpf. Prior to blood circulation, *L-plastin*-positive cells are found exclusively in the yolksac and in the mesenchyme of the head (Fig. 8Q,R). Then at 28 hpf, a distinct group of 20-30 *L-plastin*-positive cells appears in the caudal part of the axial vein and the mesenchyme surrounding it (Fig. 8S, arrow), and this group expands in the following hours (Fig. 8T). These may represent either yolksac macrophages brought by the blood circulation which settled there, or a second wave of haemopoietic activity from the caudal blood island, in which hemopoietic precursors would now produce leukocytes. Outside this ventro-caudal zone, *L-plastin*-positive cells remain strikingly scarce in the whole mid-trunk to tail region at 32 and 40 hpf, our latest in-situ hybridization time point (Fig. 8T and data not shown).

Early embryonic macrophages can eradicate bacterial infections

Eliminating apoptotic corpses (Willett et al., 1999) may not be the sole function of early embryonic macrophages. A day or so after macrophages appear, the embryo hatches and becomes directly exposed to the outer environment. Yet it still has no lymphocytes to neutralize possible microbial invaders (Willett et al., 1999). We therefore set out to test if macrophages alone could cope with a bacterial infection. We injected a large dose of either gram-negative (*E. coli*) or gram-positive (*B. subtilis*) live bacteria in the blood of 30 hpf embryos.

Within 15 minutes of *E. coli* injection, most macrophages were covered with bacteria, which adhered specifically to them

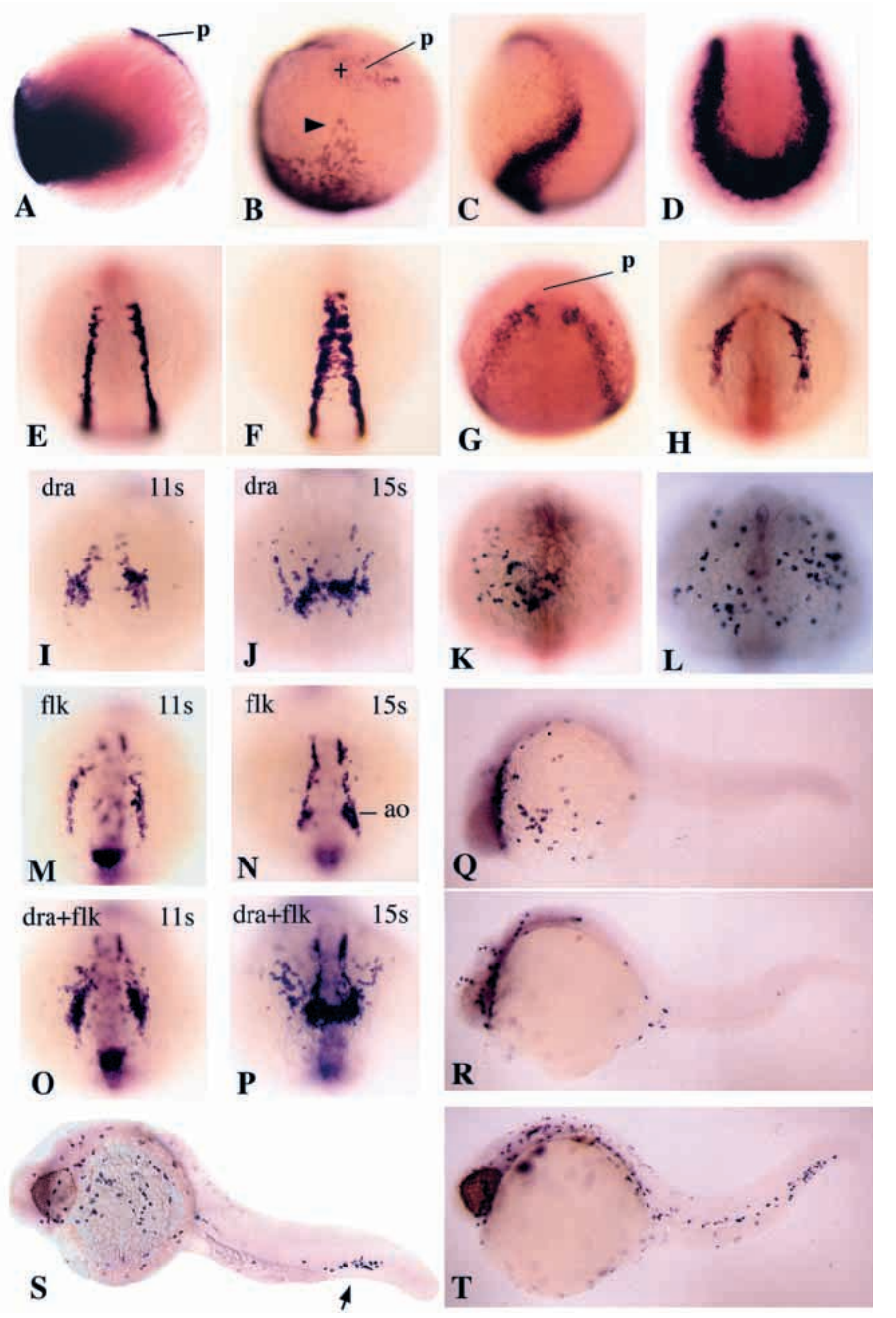

Fig. 8. Expression patterns of the *draculin* and *L-plastin* genes in the zebrafish embryo. (A-K) Expression of the *draculin* gene. (A-C) Gastrulation and early segmentation period, lateral view, animal pole on top, dorsal side to the right. (A) 75% epiboly; *draculin* is expressed in a large domain of ventral and ventro-lateral hypoblast, and in the borders of the prechordal plate (p). (B) 90% epiboly; this embryo was slightly tilted (a cross marks the animal pole) to make the prechordal plate (p) visible; the *draculin* expression domain displays a tip towards the animal pole that will become anterior lateral mesoderm. (C) 3-somite stage; *dra* is no longer expressed in the prechordal plate; two *dra* domains become apparent in lateral mesoderm: a larger one posteriorly, and a smaller one anteriorly. (D-K) Segmentation period, dorsal view, anterior to the top. (D-F) Posterior *dra* expression domain at 3-somite (D), 8-somite (E) and 13-somite (F) stages. (G-K) Anterior *dra* expression domain at 3-somite (G), 8-somite (H), 11-somite (I), 15-somite (J) and 20-somite (K) stages. (M,N) Anterior *flk* expression at 11-somite (M) and 15-somite (N) stages; the bottom spot centered on the midline is not in lateral mesoderm but in the brain. (O,P) Anterior expression of *dra+flk* at 11-somite (O) and 15-somite (P) stages; ao, aortic arch primordia. (L,Q-T) Expression of the *L-plastin* gene. (L) Dorsal view, anterior to the top, at 20-somite stage. (Q-T) Lateral view at 24 hpf (30-somite stage, Q,R), 28 hpf (S) and 32 hpf (T); the focus is on the yolksac in Q and on the embryo in R,T. In S, differently focused pictures were fused electronically to show *L-plastin*-positive cells in the embryo and yolksac simultaneously; the arrow shows the newly appeared caudal group of *L-plastin* positive cells.

and not at all to erythroblasts, and phagocytosed them rapidly (Fig. 9A,C,D). Within 3 hours (or less, upon injection of lower doses of bacteria) the blood was cleared from bacteria. Full digestion of the bacteria inside the macrophages was achieved over the next few hours (Fig. 9J,K). All embryos survived and completed their development normally.

Upon injection of an equally high dose of *B. subtilis*, the initial response was the same as with *E. coli*: adhesion of bacteria to macrophages, followed by their rapid ingestion (Fig. 9B,E,F). Then it differed. The vacuoles became much more prominent than with *E. coli*, probably for two reasons: the individual phagosomes rapidly fused into a single one, which remained full of apparently intact *B. subtilis* for several hours (Fig. 9G), probably reflecting greater difficulty in destroying this bacterium than *E. coli*. By 5 hours post injection (p.i.), 95% of the macrophages showed a similar big bacteria-filled vacuole. But only two out of seven injected embryos had cleared their blood of bacteria by this time. For these two, full digestion of the ingested bacteria needed more time than with *E. coli*, but by 17 hours, it was complete, and the two embryos developed normally. The other five embryos, which were not able to clear their blood by 5 hours p.i. despite intense phagocytosis, were overflowed with *B. subtilis* that invaded all the subcutaneous space and apparently proliferated there, and the embryos died soon after. With a fourfold lower dose of bacteria, all embryos could clear the bacteria and survived.

Unexpectedly, once challenged with bacteria, either *E. coli*

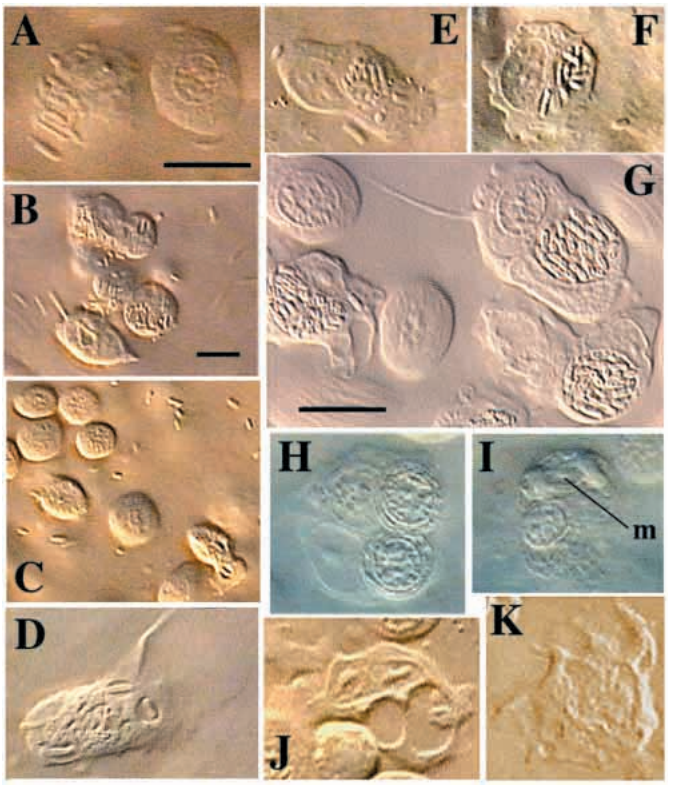

Fig. 9. Elimination of intravenously injected *E. coli* or *B. subtilis* by macrophages in 30 hpf embryos. (A) 20 minutes post intravenous injection (p.i.): *E. coli* bacteria massively stick to the surface of a macrophage, and not at all to the adjacent erythroblast. (B-F) 20 minutes (B,E,F) or 90 minutes (C,D) after injection of *B. subtilis* (B,E,F) or *E. coli* (C,D), the blood contains many bacteria; most macrophages contain many small vacuoles containing one or a few bacteria; some of them (D-F) already have several bacteria in a few vacuoles. (G) 5 hours post-injection of *B. subtilis*. The blood is cleared from bacteria; macrophages are full of bacteria gathered in a single large vacuole, which compresses and deforms the adjacent cell nucleus. One macrophage shown here has just engulfed a living erythroblast. (H-K) 5 hours after *E. coli* injection, there are no more bacteria in the blood, and almost none any more in macrophages. (H,I) A macrophage that engulfed at least five erythroblasts shown at two different foci. One of them (m), visible in I, was engulfed while undergoing mitosis. (J,K) Many macrophages now show an activated morphology: large, empty vacuoles, and greatly expanded ruffling. Bars, 10 μm; (B,C) are at the same magnification, given by the scale bar in B; A and D-K are at higher magnification, bars in A and G.

or *B. subtilis*, macrophages not only phagocytosed the bacteria, but 3-5 hours after the bacterial injection, they also began to phagocytose living, apparently healthy erythroblasts, something never done in the normal uninfected embryo (Fig. 9G-I). They even engulfed and digested dividing erythroblasts in anaphase/telophase (Figs 9I, 10I). This new behaviour correlated with an overall change in the morphology of most macrophages, towards a highly lobulated, ready-to-engulf cell surface (Fig. 9J,K).

Attraction of macrophages to sites of bacterial infection

In the blood, elimination of bacteria does not require active migration from the macrophages; bacteria stick to them, are engulfed and destroyed. We set out to test whether the macrophages could sense the presence of bacteria elsewhere in the embryo, and migrate there to destroy them.

We injected bacteria in one of the two closed body cavities available: in the pericardial cavity, at the 30-somite stage (1-2 hours before the onset of blood circulation), and in the fourth ventricle of the brain, at the 24-somite stage. At these respective stages, there are a few or no macrophages in the pericardial cavity, and none in the fourth ventricle of uninfected embryos.

In all experiments, the outcome was the same: 2 hours after injection of bacteria, the injected cavity was still full of

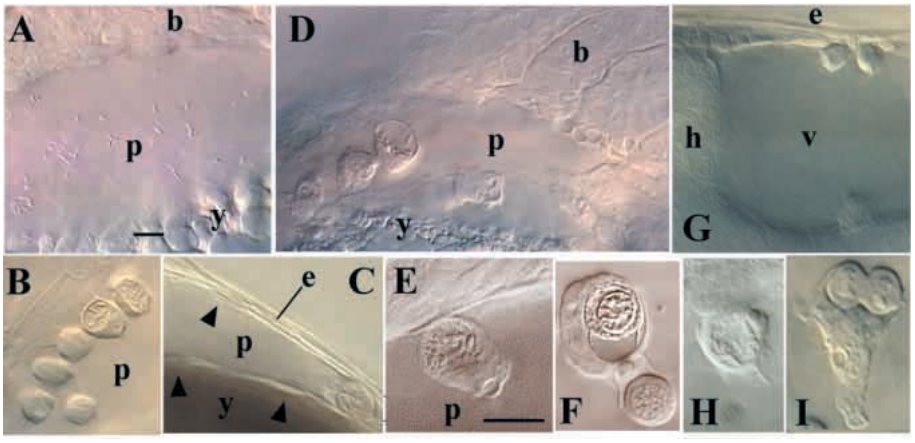

Fig. 10. Attraction of macrophages to sites of bacteria delivery outside the blood. (A-C) Injection of *B. subtilis* in the pericardial cavity at 25 hpf. (A) 1 hour post-injection (p.i.), the pericardial cavity (p), beneath the branchial arches (b), contains numerous bacteria and no phagocyte. (B) 6.5 hours p.i., the pericardial cavity now contains no more free bacteria, but 35 phagocytic macrophages, such as the six shown here; the four in the lower left quadrant are not out of focus but in fast motion, because they are attached to the myocardium of the beating heart; the two upper left phagocytes are attached to the inner side of the pericardium. (C) Sagittal view of the pericardial cavity (p); arrowheads point at nuclei slightly bulging out of the very thin pericardial epithelium; in the bottom right corner, a phagocyte lies between the ventral and dorsal sides of the pericardium. e, epidermis. (D-F) Injection of *E. coli* in the pericardial cavity, at 30 hpf. (D) 6 hours p.i., the pericardial cavity contains 24 phagocytes and no free bacteria. (E) One of these phagocytes, attached to the dorsal inner side of the pericardium. (F) In the blood, macrophages have become activated phagocytes that engulf living erythroblasts, although they have not met any bacteria. (G-I) *E. coli* injection into the hindbrain (h) ventricle at 21 hpf. (G) 5 hours p.i., the ventricle (v) is devoid of free bacteria, but contains 25 highly phagocytic macrophages, three of which are visible at this plane of focus: two are anchored to the roof of the ventricle (top), and one to the second rhombomere of the hindbrain (bottom). (H) Close-up of a macrophage bound to the roof of the ventricle. (I) 9 hours p.i.; a macrophage in the blood engulfs an erythroblast in anaphase. (A-D,G) are at the same magnification; (E,F,H,I) are at the same higher magnification. Bars,10 μm.

bacteria. But 5-6 hours post injection, either the pericardial cavity or the brain ventricle was now cleared of bacteria, and contained instead 25-35 macrophages with big vacuoles containing already partially digested bacteria (Fig. 10). All injected embryos then developed normally.

Quite interestingly, in all experiments, the other macrophages that were still in the blood, even though they did not meet bacteria, had also acquired the activated morphology and behaviour, and were now phagocytosing erythroblasts (Fig. 10F,I).

DISCUSSION

We have shown that the zebrafish contains macrophage-like mononuclear phagocytes at an unexpectedly early stage, first in the yolksac by 24 hpf and then in the mesenchyme of the head and in the blood. This progressive dissemination of macrophages from the yolksac all occurs before any other type of leukocyte appears in the embryo.

These early macrophages do not arise from the well-known caudal embryonic blood island that gives rise to erythroblasts and endothelial cells, but from the ventro-lateral mesoderm of the head just anterior to the cardiac field.

At the onset of gastrulation, the progenitors of these two hemopoietic domains map to the ventral side of the late blastula/early gastrula, which we found to express a newly isolated gene, *draculin*, that encodes a zinc-finger, probably DNA-binding protein. As they become part of the converging lateral mesoderm, these two hemopoietic domains become specified by *draculin* expression.

The anterior *dra*-expressing lateral mesoderm initially also expresses *flk-1*, an early marker of the endothelial lineage. Then just as the cells immediately posterior to the *flk*/*dra*-expressing zone stop converging and start forming the cardiac primordia, the *flk* and *dra* domains become clearly different, with *dra*-expressing cells converging and then emigrating to the yolksac as single scattered cells that will become macrophages, while *flk*-expressing cells continue to converge as two thin bands that soon delineate the bilateral primordia of arterial head vessels. Thus, in its capacity to give rise to both hemopoietic and vasculogenic cells, this small piece of lateral mesoderm anterior to the cardiac field is similar to the caudal lateral mesoderm that produces erythroblasts and endothelial cells, and also to the splanchnopleural lateral mesoderm of birds and mammals (Pardanaud et al., 1996), raising the prospect that so-called hemangioblasts (Pardanaud et al., 1996) might be the common precursors of macrophages and head arterial vessels in the zebrafish embryo.

As they migrate one after another towards the yolksac, macrophage progenitors stop expressing draculin. This happens in an assymetrical way. On the right side, the cells stop expressing draculin short after they started emigrating, while on the left side, draculin-positive emigrated cells are spread over the dorsal side of the yolk (Fig. 8K, compare to 8L). This assymetry gives a clue to the external factors that maintain draculin expression in macrophage progenitors. At late blastula/early gastrula stages, draculin expression appears to be *BMP*-dependent (B. T. and C. T., unpublished). Later, at the 20-somite stage, BMP4 is expressed in the cardiac territory assymetrically, more strongly on the left than the right (Chen et al., 1997). If BMP4 protein is secreted from the heart primordium it might promote draculin expression in neighbouring cells assymetrically, as we have observed here. This suggests a direct involvment of BMP4 in the maintenance of draculin expression in anterior lateral mesoderm and emigrating macrophage progenitors.

As macrophage progenitors emigrate to the yolksac, they start expressing *leucocyte-specific plastin*, and continue to do so as they become mature macrophages. In mammals, *L-plastin* is only expressed in leukocytes; it appears to promote enhanced integrin-mediated adhesion of leukocytes in response to the environmental signals that can activate them (Jones et al., 1998). We note that the first morphological change in zebrafish macrophage precursors as they emigrate away from the midline is their trend to round up during pauses in migration, and stretch again when they carry it further (Fig. 5). This behaviour suggests that they already use L-plastin for integrin-based adhesion and motility.

As macrophage precursors accumulate in the anterior yolksac, they adopt homogeneous morphologies, becoming rounded cells with little cytoplasm and unceasing blebbing activity, which divide frequently (Fig. 3A). These cells are strongly reminiscent of mammalian hemopoietic blast cells; we call them ‘pre-macrophages’, until we learn more about their abilities and the myeloid markers that they express. Then these pre-macrophages asynchronously begin to wander, they contain more cytoplasm, and show characteristic fast motility, with large, highly dynamic lamellipodia, filopodia and complex pseudopodia (Fig. 3B,C). Since these cells already display a typically macrophagic motility but still have no phagocytic experience, we call them ‘young macrophages’.

The early cephalic branch of the hemopoietic lineage that we have described as giving rise to macrophages is surprising in at least three respects: (1) the production of macrophages and erythroid cells from such widely separate domains of the lateral mesoderm; (2) the anterior position of the macrophage territory (in vertebrates, the head is not usually considered as a site of hemopoiesis); (3) the rapid differentiation pathway of macrophages from mesenchymal progenitors, plus their retention of proliferative potential once they have differentiated.

Yet, there is evidence for each of these three aspects from previous studies in other species. Evidence for the first two comes from work in *Xenopus* and some teleosts. Using a monoclonal antibody that recognizes all leukocyte types in *Xenopus*, Ohinata et al. (1989) found non-lymphoid, macrophage-like leukocytes spread throughout the embryonic mesenchyme before the onset of blood circulation, and before the ventral blood island starts producing leukocytes. Moreover, with reciprocal grafting experiments in which they exchanged the head and body of marked embryos, as well as in cultured explants, Ohinata et al. (1990) showed that early non-lymphoid leukocytes arise entirely from the head, cut just anterior to the presumptive heart territory.

Likewise, when Colle-Vandevelde (1963) studied the location of hemoglobin-producing blood islands in various teleost embryos, she found a striking diversity among different species. In the Siamese fighting fish, the erythroid blood island was spread on the anterior aspect of the yolksac, in a pattern strikingly similar to young macrophages in zebrafish,

suggesting that in some teleosts, the cephalic hemopoietic progenitors give rise to erythroid cells (leukocytes were not examined in this study).

A third atypical feature we found was the rapid differentiation pathway of early macrophages. New macrophages in adult mammals are produced as the result of a multi-step differentiation pathway in the bone marrow, starting with a multipotential haemopoietic stem cell, that gives rise after some intermediates to a myeloid precursor. This then gives rise to both granulocyte and macrophage lineages, including the monocytic series that finally gives rise to the differentiated, post-mitotic macrophage. Macrophages are usually thought to be produced in embryonic blood islands through the same differentiation pathway, and to colonize the organs only through the blood, as monocytes, as they do in the adult (Van Furth, 1980) However, over the last decade, three laboratories, working with mouse, rat and chicken embryos, respectively, have challenged this view (Sorokin et al., 1992a,b; Cuadros et al., 1992, 1993; Takahashi et al., 1996 and references therein). Their results are strikingly similar to our findings in zebrafish. In rodents, macrophages appear in the yolksac well before any monocyte or granulocyte, suggesting that they arise from some hemopoietic stem cell through a pathway that bypasses the monocytic series. So-called 'primitive macrophages', similar to the pre-macrophages that we described here, quickly mature into 'fetal macrophages', which still display a clear proliferative potential (Takahashi et al., 1996). From the yolksac, they quickly invade the mesenchyme of the head, and from there several forming organs, in which they can be seen dividing (Cuadros et al., 1993; Sorokin et al., 1992b).

The early macrophages that we describe in the zebrafish embryo are most likely homologous to these primitive/fetal macrophages described in rodent and avian embryos.

One future goal is to know the long-term fate of these macrophages in the zebrafish. Are they replaced later by 'classical', monocyte-derived macrophages born in the hemopoietic organs of the adult, or are they long-living residents in adult tissues? Then they may constitute a sub-population of tissue macrophages with self-renewal capacity (as opposed to the post-mitotic, monocyte-derived macrophages), and possibly with a distinct physiology and sensitivity to various cytokines and chemoattractants (Sorokin et al., 1992a,b; Takahashi et al., 1996).

Not only scavengers

We found that zebrafish early macrophages phagocytose apoptotic erythroblasts, as well as apoptotic cells in the head (P. H., unpublished data). Yet it remains uncertain if they eliminate all apoptotic corpses in the embryo. Indeed, apoptotic cells are common in the brain and eyes well before these macrophages become operational. How the embryo eliminates them is unknown.

A day or so after macrophages appear, the embryo hatches, and becomes exposed to the outer environment. Yet it has no immune system. Macrophages provide an essential defence line against microbial invaders. We have found that they efficiently eradicate bacterial populations without the help of lymphocytes, which are born much later (Willett et al., 1999). Upon infection, they become activated, and so phagocytic that they now also phagocytose living erythroblasts. Our findings imply that they have cell surface receptors that can recognize both gram– and gram+ bacteria without the help of antibodies. Such receptors could be related to the mannose receptor of mammalian resident macrophages, which can recognize glycosyl motifs specific of microbial walls (Takahashi et al., 1998).

When the pericardial cavity or the fourth ventricle of the brain was injected with *E. coli* or *B. subtilis*, 25-35 macrophages came into the cavity to clear the bacteria. This is much more than the number of resident macrophages that we find on the outer surface of these cavities or inside them in uninfected embryos, especially at the times at which we injected the bacteria (P. H., unpublished data). Therefore, macrophages initially remote from the sites of infection must have been attracted there, either by chemotactic molecules emanating from the bacteria, or by cytokines released by the few macrophages initially residing close to these sites. The latter seems all the more likely that these local infections induced the morphological transformation and aggressive phagocytic behaviour of the entire macrophage population of the embryo.

Early macrophages and developmental processes

Macrophages are not only scavengers or fighters, they also secrete an impressive array of growth factors and cytokines in various situations, as well as various proteins capable of remodelling the extracellular matrix (Auger and Ross, 1992). They might therefore be involved in regulating aspects of organogenesis.

Firstly, we observed that macrophages in the yolksac circulation valley interact closely with erythroblasts, sometimes seemingly almost engulfing them, but then releasing them back to the circulation. This intimate interaction resembles the nursing role of mammalian macrophages towards immature erythroid cells, although in the zebrafish embryo it does not take place in a tissue environment as structured as the bone marrow or even the hemopoietic fetal liver of mammals (Crocker and Milon, 1992). The interaction of young macrophages and proerythroblasts in the zebrafish yolksac might be important for the maturation of both cell types.

Secondly, it is known that macrophages can promote angiogenesis (Auger and Ross, 1992). Since we found that they invade the mesenchyme of the head about 4 hours prior to its first vascularization (Rieb, 1973), they could be involved in fostering proper vascularization of the head, which soon becomes much more elaborated than in the rest of the body.

Towards a cell biology of macrophages in the live animal

Since we can easily follow individual macrophages in the live zebrafish embryo by video-enhanced DIC microscopy, we have here a unique opportunity to study their cell biology directly in the living vertebrate organism.

We noticed that macrophages in the yolksac circulation valley often adopt a typical shape (Fig. 2G-K) collectively. This may signal a change in cytokines in the microenvironment. We now know that small GTP-binding proteins Rho, Rac and Cdc42, which are key-relays of much cytokine signalling inside the cell, induce definite effects on actin-based cell protrusions. In mouse macrophages, Cdc42 induces the

formation of filopodia, Rac induces lamellipodia and membrane ruffling, while Rho induces cell rounding (Allen et al., 1997). Thus, we may soon become able to read the swiftly changing morphologies of macrophages in these terms, and use these wandering cells as sensitive, readily readable probes of their fluctuating cytokine environment.

P. H.'s contribution to this work was carried out in J. F. Nicolas' laboratory. We are grateful to G. Milon and P. Berche for suggesting that we inject bacteria in the embryo, to J. C. Bénichou for his help with the Adobe Photoshop software, and to T. Schilling for his help in the preparation of the manuscript. We also thank V. Heyer and T. Steffan for technical assistance, and O. Nkundwa and A. Karmim for maintenance of fish. This work was supported by the Institut National de la Santé et de la Recherche Médicale (C.T. and B.T.), the Centre National de la Recherche Scientifique, the Hôpital Universitaire de Strasbourg (C.T. and B.T.), the Association pour la Recherche sur le Cancer and the Ligue Nationale contre le Cancer.

REFERENCES

Al-Adhami, M. A. and Kunz, Y. W. (1977). Ontogenesis of haematopoietic sites in *Brachydanio rerio*. *Dev. Growth Differ.* **19**, 171-179.

Allen, W. E., Jones, G. E., Pollard, J. W. and Ridley, A. J. (1997). Rho, Rac and Cdc42 regulate actin organization and cell adhesion in macrophages. *J. Cell Sci.* **110**, 707-720.

Auger, M. J. and Ross, J. A. (1992). The biology of the macrophage. In *The Macrophage*. (ed. C. E. Lewis and J. D. McGee), pp. 1-74. Oxford University Press, Oxford.

Cannon, G. J. and Swanson, J. A. (1992). The macrophage capacity for phagocytosis. *J. Cell Sci.* **101**, 907-913

Chen, J. N., van Eeden, F. J. M., Warren, K. S., Chin, A., Nusslein-Volhard, C., Haffter, P. and Fishman, M. C. (1997). Left-right pattern of cardiac BMP4 may drive assymetry of the heart in zebrafish. *Development* **124**, 4373-4382

Colle-Vandevelde, A. (1963). Blood anlage in teleostei. *Nature* **198**, 1223.

Crocker, P. R. and Milon, G. (1992). Macrophages in the control of hematopoiesis. In *The Macrophage* (ed. C. E. Lewis and J. O. McGee), pp. 115-156. Oxford University Press, Oxford.

Cuadros, M. A, Coltey, P., Nieto, M. C. and Martin, C. (1992). Demonstration of a phagocytic cell system belonging to the haemopoietic lineage and originating from the yolksac in the early avian embryo. *Development* **115**, 157-168

Cuadros, M. A., Martin, C., Coltey, P., Almendros, A. and Navascués, J. (1993). First appearance, distribution, and origin of macrophages in the early development of the avian central nervous system. *J. Compar. Neurol.* **330**, 113-129.

Detrich III, H. W., Kieran, M. W., Chan, F. Y., Barone, L. M., Yee, K., Rundstadler, J. A., Pratt, S., Ransom, D. and Zon, L. I. (1995). Intraembryonic haematopoietic cell migration during vertebrate development. *Proc. Natl. Acad. Sci. USA* **92**, 10713-10717.

Fouquet, B., Weinstein, B., Serluca, F. and Fishman, M. (1997). Vessel patterning in the embryo of the zebrafish: guidance by notochord. *Dev. Biol.* **183,** 37-48

Hayden, J. H. and Allen, R. D. (1984). Detection of single microtubules in living cells: particle transport can occur in both directions along the same microtubule. *J. Cell Biol.* **99**, 1785-1793.

Jones, S. L., Wang, J., Turck, C. W. and Brown, E. J. (1998). A role for the actin-bundling protein L-plastin in the regulation of leukocyte integrin function. *Proc. Natl. Acad. Sci. USA* **95**, 9331-9336

Kimmel, C. B., Ballard, W. W., Kimmel, S. R., Ullmann, B and Schilling, T. F. (1995). Stages of embryonic development of the zebrafish. *Dev. Dyn.* **203**, 253-310.

Ohinata H., Tochinai, S. and Katagiri, C. (1989). Ontogeny and tissue distribution of leukocyte-common antigen bearing cells during early development of *Xenopus laevis*. *Development* **107**, 445-452

Ohinata H., Tochinai, S. and Katagiri, C. (1990). Occurrence of non-lymphoid leukocytes that are not derived from blood islands in *Xenopus laevis* larvae. *Dev. Biol.* **141**, 123-129

Pardanaud L., Luton, D., Prigent, M., Bourcheix, L., Catala, M. and Dieterlen-Lièvre, F. (1996). Two distinct endothelial lineages in ontogeny, one of them related to hemopoiesis. *Development* **122**, 1363-1371

Rieb, J.-P. (1973). La circulation sanguine chez l'embryon de *Brachydanio rerio*. *Ann. Embryol. Morph.* **6,** 43-54

Sorokin, S. P., McNelly, N. A. and Hoyt, R. F. (1992a). CFU-rAM, the origin of lung macrophages and the macrophage lineage. *Am. J. Physiol.* **263**, L299-L307

Sorokin, S. P., Hoyt, R. F., Blunt, D. G. and McNelly, N. A. (1992b). Macrophage development: II. Early ontogeny of macrophage populations in brain, liver and lungs of rat embryos as revealed by a lectin marker. *Anat. Rec.* **232**, 527-550

Strehlow, D., Heinrich, G. and Gilbert, W. (1994). The fates of the blastomeres of the 16-cell zebrafish embryo. *Development* **120**, 1791-1798.

Takahashi, K., Naito, M. and Takeya, M. (1996). Development and heterogeneity of macrophages and their related cells through their differentiation pathways. *Pathol. Int.* **46**, 473-485.

Takahashi, K., Donovan, M. J., Rogers, R. A. and Ezekowitz R. A. (1998). Distribution of murine mannose receptor expression from early embryogenesis through to adulthood. *Cell Tissue Res.* **292**, 311-323.

Thisse, C., Thisse, B., Schilling, T. F. and Postlethwait, J. H. (1993). Structure of the zebrafish *snail1* gene and its expression in wild-type, *spadetail* and *no tail* mutant embryos. *Development* **119**, 1203-1215.

Van Furth, R. (1980). Cells of the mononuclear phagocyte system. Nomenclature in terms of sites and conditions. In *Mononuclear Phagocytes: Functional Aspects*, part I (ed. R. van Furth), pp. 1-30. Martinus Nijhoff Publishers, La Hague.

Westerfield, M. (1995). *The Zebrafish Book.* University of Oregon Press, Eugene.

Willett, C. E., Cortes, A., Zuasti, A. and Zapata, A. G. (1999). Early hematopoiesis and developing lymphoid organs in the zebrafish. *Dev. Dyn.* **214**, 323-336.